Technical Article

Electromagnetic hysteresis modelling: from material science to finite element analysis of devices

***Abstract* — This paper deals with numerical modelling techniques for hysteresis properties in magnetic materials. Physical and phenomenological models are discussed. First some basic hysteresis properties are described in order to proceed gradually to more sophisticated models, which can be included into finite element formulations. Scalar and vector hysteresis models are considered. We distinguish between rate-independent and rate dependent material behaviour.**

I. Introduction

The phenomenon of hysteresis has been observed for a long time in many different areas of science and engineering. Examples of hysteresis in material systems include mechanical hysteresis, magnetic hysteresis, ferroelectric hysteresis and many others. In some applications hysteresis can be employed for a useful purpose. Such is the case in systems relying on permanent magnets and in magnetic recording. In other cases such as positioning systems, electrical machines, hysteresis phenomena are often unwanted and consequently must be avoided as much as possible.

In general two types of modelling techniques are used to describe hysteresis processes: physical modelling and phenomenological modelling. In physical modelling, the basic processes involved are simulated in order to be able to describe the basic magnetizing modes. In phenomenological models, the gross behaviour of the material is described mathematically by generating curves, following predefined rules, for the material properties. The latter models are often computationally more efficient than the former, but they do not give any insight into the physical principles involved.

For the design of electromagnetic devices, accurate evaluations of the magnetic field patterns in the device are often essential for a realistic prediction of the performance characteristics of the device. Consequently, in many cases, the magnetic field computations should account for the precise features of the magnetic materials used, including the hysteresis effects. At this point, the macroscopic properties, described by phenomenological models are coupled with the Maxwell's equations so as to obtain accurate solutions for electromagnetic field problems.

Hysteresis modelling becomes even more important when one aims at the evaluation of properties directly related to hysteresis processes, e.g. the calculation of iron losses in electromagnetic devices. We recall that the hysteresis loss is related to the fact that the relationship between the magnetic induction vector $\underline{B}$ and the magnetic field vector $\underline{H}$ in the material depends on the history of the magnetic field. For these cases a phenomenological hysteresis model describing the $\underline{B}$-$\underline{H}$-relation is sufficient as long as the desired accuracy is obtained.

For other applications, such as magnetic hysteretic non-destructive testing (NDT), there is a preference for a physical hysteresis model, or a model the parameters of which can be directly related to microstructural features of the material. It is clear that a hysteresis model that has to be used for interpretation of NDT results should have at least a few parameters that are directly related to the metallurgical properties of the material. Changes in the material microstructure lead to a modification of the mechanical properties, which should be identified by the changes of the magnetic hysteresis properties, or the limited number of material parameters defined in the hysteresis model.

Finally, one must distinguish between scalar hysteresis models and vectorial hysteresis models. Indeed, depending on the application, the flux pattern may be unidirectional, i.e. the direction of the magnetic field or the magnetic induction is fixed but the amplitude is changing continuously. For other applications, e.g. in rotating electrical machines, a non-negligible part of the magnetic fields has a rotational character, i.e. the amplitude as well as the direction of the magnetic field and the magnetic induction vector change continuously.

The aim of this paper is to describe the basic principles of hysteresis modelling and discuss some aspects in more detail.

II. Some basic hysteresis properties

Hysteresis modelling handles the problem of how to construct (predict) the transition curves, which correspond to any changes of the magnetic field H. In spite of the variety of characteristics among different magnetic materials some general features are observed in their magnetization processes. These features have been described already in 1905 [1] and are known as Mandelung's rules. Considering the hysteresis curves in Fig.1, these experimentally established rules can be stated as follows:

1) The path of any transition (reversal) curve is uniquely determined by the coordinates of the reversal point, from which this curve emanates.

2) If any point 4 of the curve 3-4-1 becomes a new reversal point, then the curve 4-5-3 originating at point 4 returns to the initial point 3 ('return-point-memory')

3) If the point 5 of the curve 4-5-3 becomes the newest reversal point and if the transition curve 5-4 extends beyond the point 4, it will pass along the part 4-1 of curve 3-4-1, as if the previous closed loop 4-5-4 did not exist at all ('wiping-out property')

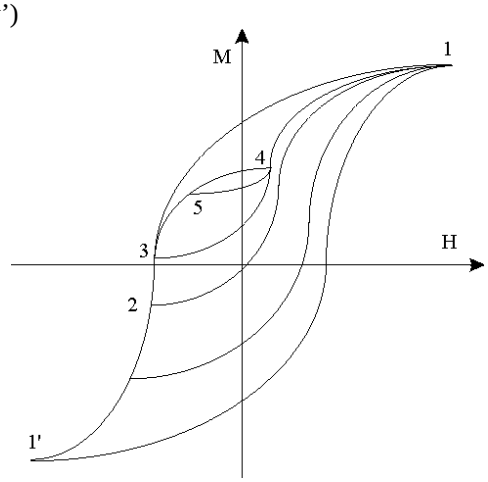

Fig.1: Transition curves illustrating Mandelung's rules

The closed loop 4-5-4 is called a minor loop.

III. Scalar Preisach Modelling

One of the most widely used models for magnetic hysteresis is the Preisach model described in [2] or extensions of the original model. All these Preisach type models have a common feature: the magnetization curves are constructed as a superposition of simple hysteresis non-linearities, i.e. rectangular loops, defined by an 'up' switching field α to the *+1* state and a 'down' switching field β to the *–1* state, $\alpha>\beta$. Advanced hysteresis models, such as the Preisach models should reproduce all main features of magnetization, including the 'return-point-memory' and the 'wiping-out' property.

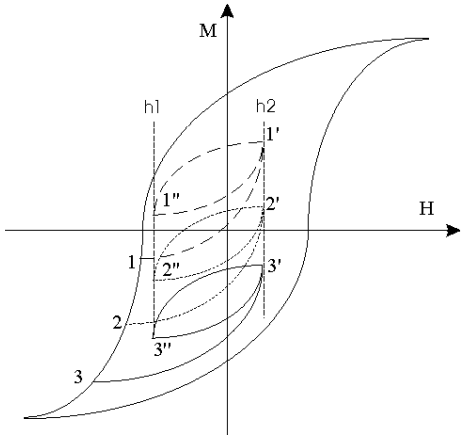

Fig.2: Magnetization curves illustrating the congruency properties

Firstly, the classical Preisach model describes rate-independent (quasi-static) hysteresis. Indeed, the hysteresis memory state at each time point is determined only by the extreme values (maxima and minima) of the field strength history ('return-point-memory'). The relevant extreme value H_{extr} is the last one stored in memory. The closing of a minor loop deletes from memory the maximum and minimum *H*-values associated with this minor loop ('the wiping-out property'). When no extreme values are present in memory, the virgin magnetization curve is followed. The third important property of the classical Preisach model is the 'congruency property', see Fig.2. It states that *BH*-loops between two fixed extreme field values h_1 and h_2 are independent of the induction level *B*. In the classical Preisach model, the magnetization *M* corresponding with the magnetic field *H* and its history H_{hist} is obtained as the superposition of a reversible $M_{rev}(H)$ part and an irreversible part $M_{irr}(H, H_{hist})$, the latter given by

$$M_{irr} = \int_{-\infty}^{+\infty} da \int_{-\infty}^{a} db\ P(a,b)\, f(a,b,H,H_{hist}) \quad (1)$$

Here, the $f(a,b,H,H_{hist})$ has the value *+1* or *–1*, respectively when the Preisach dipole with parameters α,β is in the 'up' state or the 'down' state at the considered time point. The density of these dipoles is represented by the Preisach distribution function $P(\alpha,\beta)$ (PDF), characterizing the material. M_{irr} is determined by the magnetic state of all elementary dipoles, which, in turn, depends on the magnetic history of the material.

Somewhat simultaneously, hysteresis effects were studied by D.H Everett [3]. The Everett function $E_v(H_1,H_2)$ takes as value the variation of the magnetization when varying the magnetic field *H* from H_1 to H_2 without evading extremal values of the magnetic field from the memory. The function has a positive value in case of an ascending branch and a negative value in the opposite case. The magnetization *M* is given by:

$$M(H(t)) = \frac{1}{2}E_v(-H_1,H_1) + \sum_{i=2}^{N} E_v(H_{i-1},H_i) \quad (2)$$

$H_1, H_2, H_3, \ldots H_{N-1}$ are the extreme values of the magnetic field in memory at time point *t* and $H_N=H(t)$. It is well known that the Everett function $E_v(H_1,H_2)$ can be identified experimentally using e.g. Epstein frame combined with an acquisition system and power amplifier able to enforce a quasi-static current of any shape in the excitation winding. As the Everett function $E_v(H_1,H_2)$ is directly related to the Preisach function [4]:

$$P(a,b) = -\left.\frac{\partial^2 E_v}{\partial H_1 \partial H_2}\right|_{\substack{H_1=a \\ H_2=b}} \quad (3)$$

Eq.(3) may be used to identify the Preisach distribution function [5].

The density of the dipoles is represented by the Preisach distribution function $P(a,b)$, characterizing the material. The resulting magnetization *M* of the entire material is obtained from the accumulated magnetization of all the dipoles. In order to quantify how the distribution changes due to a variation of grain size or of dislocation density, a Lorenzian PDF is considered [6]. It was shown in [6], that a Lorenzian distribution is a suitable distribution function to describe the experimentally obtained magnetization loops of steels. In particular, the physical information contained in the longer tail of the Lorenzian distribution enables a better fit to experimentally obtained hysteresis data than other type of distributions, for example the Gaussian distribution.

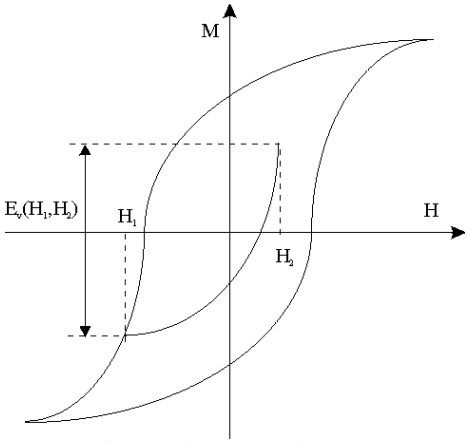

Fig.3: Definition of the Everett function $E_v(H_1,H_2)$

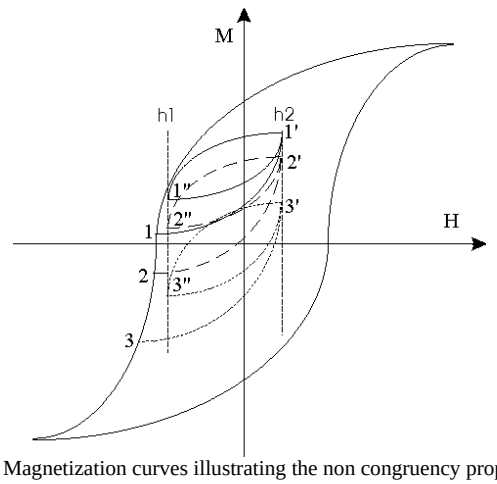

Fig.4: Magnetization curves illustrating the non congruency properties

The classical Preisach model has the 'congruency property' and thus is inapplicable to many real materials as experimentally non-congruent minor loops between two fixed extreme field values h_1 and h_2 are often observed.
Moreover, the phenomenon of accommodation or reptation has been observed in many magnetic materials [7]. This phenomenon states that it takes many cycles before a minor hysteresis loop closes upon itself, see Fig.5. In the classical Preisach model this is immediately, i.e. the classical Preisach formalism results in an immediate formation of the stable minor hysteresis loops after only one cycle of back and forth input variations between two consecutive extremum values.

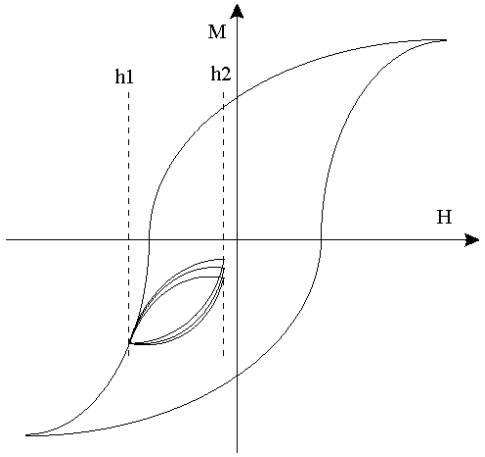

Fig.5: Magnetization curves illustrating the accommodation or reptation processes

The accommodation processes are different from after-effects that refer to the drift in magnetization while the applied magnetic field is held constant, since accommodation requires a change in the applied field to occur.
In [8] the 'moving Preisach model' and the 'product Preisach model' were introduced in order to be able to describe the experimentally observed non-congruency and accommodation. In the former model, the magnetic field *H* as input of the model is replaced by an effective field $H_e=H+kM$ while in the latter the Preisach function *P(a,b)* in Eq.(1) is replaced by *R(M)P(a,b)* with *R(M)* an even function of the magnetization *M*. Both extended models, the so called output-dependent Preisach models, were compared in [9]. An important consequence of the moving Preisach model is the 'linear skew congruency': congruent minor loops are connected by a line whose slope is –1/k, see Fig.6.
Experiments show that the moving Preisach model is actually able to give a good description of hysteresis phenomena in magnetic recording [10] as well as in metallic materials [11].

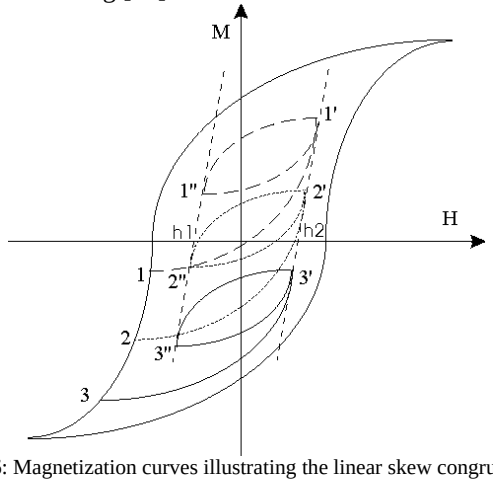

Fig.6: Magnetization curves illustrating the linear skew congruency

A question that has been widely debated is whether the Preisach model mathematical structure is able to describe the physical aspects of ferromagnetic hysteresis. For this reason, it is often convenient to describe the Preisach formalism in terms of the 'interaction fields' $h_i=(\alpha+\beta)/2$ and the critical fields $h_c=(\alpha-\beta)/2$. In [12] it is described in detail that the interpretation of hysteresis data through the moving Preisach model should permit one to separate pinning and interaction effects, described by $P(\alpha,\beta)$, and associated with the inherent disorder of ordinary materials (fluctuations in particle size, shape orientation, presence of grain boundaries,…) from mean field interactions, described by the moving parameter *k*. A valuable approach to the characterization of magnetic interactions is represented by the so-called Henkel plot [13]. Moreover, it has been found in [12] that the moving parameter k can be associated with the longitudinal magnetostatic interactions responsible for the Barkhausen effect.
For magnetic recording material, the moving Preisach model has even been extended to a complete-moving hysteresis model [14]. It is shown that the reversible as well as the irreversible components of the magnetization are Preisach state-dependent and are coupled through the feedback parameter *k*. Therefore, in the complete moving Preisach model, the rectangular hysteresis loop for one dipole is replaced by a more realistic, non-rectangular hysteresis loop. This extension results in a non-linear skew congruency property, i.e. the locus created by congruent minor loops is not a straight line. The parameter identification of the complete moving Preisach model is described in [15].
The product model [16], [17] computes the total magnetization M when the magnetic field is increasing according to

$$\frac{dM}{dH} = R(M)\left[b + \int_{H_0}^{H} P(H,b)\,db \right] \qquad (4)$$

The non-congruency function R(M) in the product model is an even function of M/M_s. It also has the turn-off property, that is, it is equal to zero when the magnitude of M is equal to saturation magnetisation M_s. This property prevents the magnetization from exceeding saturation for any magnetization process. The integral of Eq. (4) corresponds to the irreversible magnetization while the parameter b in (4) corresponds to a reversible process. Just like H_e in the complete moving Preisach model, the parameter b may be function of both *H* and *M*.
Finally, notice that relaxation effects in magnetic materials and their influence on the hysteresis behaviour of these materials have been studied in detail in literature. In [18] the connection between hysteresis and time effects due to thermal relaxation is studied in the frame of Preisach hysteresis modelling. Relaxation effects are generally studied by measuring the magnetization decay at constant field (magnetic viscosity, after effects). The state line [19] in the Preisach model, splitting up the Preisach plane in a sub region of dipoles in the 'up'-state and a sub region of dipoles in the 'down'-state, is not defined only by the extreme values of the magnetic field kept in memory of the material but by the whole field history H(t).
In [20] the modelling of after effect phenomena in hysteretic systems using Preisach type models is driven by stochastic inputs. Thermal perturbations, which result in the gradual loss of memory in hysteretic systems, are modelled by discrete and continuous time stochastic inputs. This temporal loss of memory of a hysteretic can be of practical significance in various engineering applications where hysteresis is utilized.

One important example is the magnetic storage where the viscosity effect is important as far as the time reliability of recorded information is concerned.

IV. The Differential Equation Based Hysteresis Model

The Hodgdon's model [21] assumes a constitutive relation between H and B given by the differential equation:

$$\frac{dH}{dB} = a\ \mathrm{sgn}\left(\frac{dH}{dt}\right)\left[f(B) - H\right] + g(B) \qquad (5)$$

With a proper choice of α and of the material functions f and g, it is possible to describe hysteresis loops of various ferromagnetic materials. The most interesting properties of this model concern the behaviour of the minor loops. If *H* oscillates between a minimum and maximum value of the magnetic field H, the resulting magnetization loop moves towards a stable loop, independent of the initial state. This behaviour is experimentally observed on some type of materials and is known as the already mentioned accommodation phenomenon.

Another well known differential equation based hysteresis model is the Jiles-Atherton model [22], [23]. The proper equations are obtained from the principle that the total energy supplied to the ferromagnet may be split into two terms: the energy dissipated against pinning (hysteresis loss) and the change in energy due to the change in magnetization of the solid which may be considered reversible. [24]
In this model the total magnetization *M* is the sum of a reversible (M_{rev}) and an irreversible (M_{irr}) component. These components are given by

$$M_{rev} = c_j\left(M_{an} - M_{irr}\right) \qquad (6)$$

$$M_{irr} = M_{an} - \frac{k_j d}{m_0}\frac{dM_{irr}}{dH_e} \qquad (7)$$

Here, M_{an} is the anhysteretic magnetization, and where H_e is the effective magnetic field inside the material, i.e. $H_e = H + \alpha_j M_{an}$. The anhysteretic curve is often described by the Langevin function and the parameters M_{sj}, a_j. The number d, taking the value +1 or –1, depending on whether H is increasing or decreasing, corresponds mathematically to the hysteresis. Eq.(6) describes the reversible processes: reversible domain wall bowing, reversible translation and rotation. In [25] it is shown how the material parameters M_{sj}, c_j, a_j k_j, and a_j can be obtained starting from the following magnetic properties: the initial normal susceptibility, the initial anhysteretic susceptibility, the coercivity, the differential susceptibility at remanence and the coordinates H_m, M_m of a loop tip, together with the differential susceptibility of the initial magnetization curve at the loop tip. However, using (6) and (7) results in unrealistic minor order loops, e.g. negative values for the differential permeability. Therefore, a generalization of the theory of hysteresis was described in [26] which allows self consistent description of all forms of minor hysteresis loops without the need to invoke any additional parameters. Volume fractions for the irreversible and the reversible components were introduced.

Although the Jiles-Atherton model and the Preisach models are defined in a completely different way, in [27] it is shown that by referring to fundamental energy relations, which can be used to describe the models in terms of stored and dissipated energy, one is able to derive the fundamental expressions of magnetization laws of the Jiles-Atherton model by applying a physical meaningful set of assumptions to the Preisach model.

V. Dynamic Scalar Hysteresis Models

In previous sections the presented hysteresis models are static in nature. The term 'static' implies that in these models only past input leave their mark upon the values of output, while the speed of input variations has no influence on the hysteresis branching. The magnetization curves, or hysteresis loops of ferromagnetic materials change as a function of the frequency and waveform of the applied magnetic field. There are many hysteresis models which take dynamic broadening of the hysteresis loop with frequency into account. Most of these are built on a static hysteresis model.
The dynamic model of Jiles [28], [29] is based on his static hysteresis model [24]. The dynamic model of [28] is based on the second order linear differential equation of motion of domain walls, which is averaged to describe the behaviour of the whole material. The result is a differential equation of second order describing the displacement magnetization $\Delta M = M(t) - M_0(H)$ where $M_0(H)$ is the locus of points on the DC hysteresis curve. The frequency dependent hysteresis curves therefore consist of two independent contributions to the magnetization. These are the dc hysteresis curve, which represents the locus of equilibrium magnetization as a function of the field and the displacement magnetization, which obeys the damped harmonic motion equation.
The main idea behind the dynamic Preisach model described in [19] is to introduce the dependence of Preisach functions on the speed of change of the magnetization dM/dt. There, it is suggested to use a power series expansion for the Preisach function with respect to dM/dt in order to simplify the identification of the material parameters. According to that model, the dynamic effects can be described by a differential equation for dM/dt. By retaining a limited number of terms in the power series expansion, the order of the differential equation for dM/dt can be chosen according to the accuracy needs with respect to measurements results.
In [30] a generalized scalar Preisach model is presented where rate-dependent effects are introduced by assuming that the switching of each elementary Preisach dipole is not instantaneously, as is the case for the standard Preisach model, but at a finite rate controlled by the external magnetic field. The basic consequence of this assumption is that the width of the hysteresis loop increases with increasing magnetizing frequency. In soft magnetic materials the proposed generalization has a direct physical interpretation in terms of domain wall dynamics [31]. Moreover, the results of this rate-dependent Preisach model could be directly related to the statistical loss theory [32], [33] and physically interpreted [34]. A general approach to the calculation of iron losses in soft magnetic materials is based on the separation of losses into three components: the hysteresis losses P_h, the classical eddy current losses P_c and the excess losses P_e. Each component has its own peak induction and frequency dependence [35]. In [30] a switching speed proportional to the difference between *H(t)* and the elementary loop switching fields α or β is described, resulting in an excess loss term varying according to the $f^{3/2}$ law. In [36] and [37], this switching law was generalized and related to the $n(H_{exc})$ –

characteristic defined in the statistical loss theory. In [38], [39] a model was presented taking into account all dynamic effects. The model is based on the equation:

$$P_{tot}(t) = P_{hyst}(t) + P_{dyn}(t) = \frac{dB(t)}{dt} H_{tot}(t) = \frac{dB(t)}{dt}\left(H_{hyst}(t) + H_{dyn}(t)\right) \quad (8)$$

directly related to the statistical loss theory. For a given induction B – the mean induction in the thickness of the sheet-, the magnetic field H_{tot} - at the surface of the sheet – has two components: a DC-contribution $H_{hyst}(t)$, directly related to a rate-independent Preisach model and a dynamic contribution $H_{dyn}(t)$ describing all dynamic processes (classical eddy current losses and excess losses), see Fig.7. The dynamic behaviour of the material is described by the function $H_{dyn}(B(t), dB(t)/dt)$ which can be identified experimentally [39].

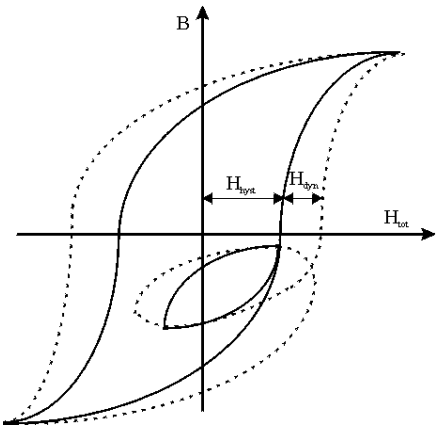

Fig.7: Static and dynamic magnetization curves illustrating two components of the total field H_{tot}

VI. VECTOR HYSTERESIS MODELLING

The previous discussions were limited to scalar models. However, in many cases the magnetizing processes is vectorial in nature.

The magnetization processes, under rotational fields, undergo several changes at different magnetization levels: at low fields 180° domain wall motion prevails, while at intermediate fields the role of the 90° walls becomes important. Finally at high induction level the local magnetization inside a grain can deviate from the easy direction for coherent rotation. The coherent rotation process is in fact responsible for the decrease of rotational losses at high fields, when the magnetizing vector saturates and becomes parallel to the field. Aiming at the development of a physically based vector hysteresis model includes the construction of a model able to describe domain wall motion and coherent rotation and able to depict the transition from domain wall motion to coherent rotation.

This makes the design of a proper vector hysteresis model a difficult task. One approach to vector hysteresis is the particle assembly approach. In [40] vector hysteresis was treated by considering the material consisting of an assembly of identical, non-interacting, single-domain uniaxial particles. This model was extended in [41] and the switching criterium was modified to that derived from the Stoner-Wohlfarth model [42].

There has been numerous attempts to generalize the original Preisach model to bring it closer to the physical reality by including vectorial field magnetization relations. Several models have been proposed to introduce a vector component in Preisach modelling. In general, vector hysteresis models have to obey the 'saturation property': the magnetization must be limited to saturation for any magnetizing process, and the 'loss property': for large rotating fields, the hysteresis loss should go to zero.

A vector Preisach model of great generality was introduced in [43]. In this model there is a set of scalar Preisach models, each one having a different magnetization direction and responding to the component of the applied field in that direction, see Fig. 8 in case the set contains two scalar Preisach models along orthogonal axes. The identification problem for both isotropic and anisotropic materials is discussed in [19].

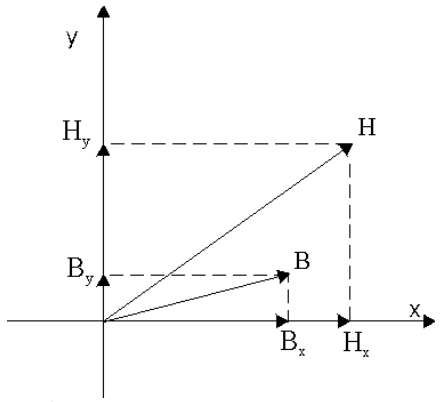

Fig.8: Principle of the 'Mayergoyz' vector Preisach model. The H-vector is projected on the axes of each scalar model in the set. In each scalar model the projection of H is used as input. The vector B is obtained as the vector sum of all contributions of B-components of the scalar models.

This vector Preisach model has been critized [44], [45] as it fails to properly describe the rotational properties of magnetic materials. In particular, for a large rotating field, every member of the scalar models must describe a complete hysteresis loop and the calculated rotational hysteresis loss reaches a constant nonzero value. The disagreements with experimental observations can be mainly traced to the inadequacy of the 'effective' input components, which cannot introduce sufficient changes in the orthogonal output components. Indeed, if the set of scalar Preisach models are permitted to be independent, then the saturation property is violated for large fields. This fact prompted further research efforts to develop new vector Preisach models. In an effort to develop a more accurate vector model, the original model of [43] was generalized by defining a new type of projection for the applied field vector on each direction corresponding with one scalar Preisach model [46]. In [47] a model was introduced in which the scalar Preisach models respond to perpendicular field components: the fundamental assumption of the proposed model is that field components perpendicular to the axis associated with a scalar Preisach model have the effect of a partial ac demagnetisation on that model. This model was based on a series of measurements that showed that when a material is magnetized in one direction, it eventually becomes demagnetised in the perpendicular direction. The degree of demagnetisation depends on the magnitude of the field, and is complete for large magnetic fields. The vector Preisach models proposed in [47] and [48] involve modification of the scalar Preisach model by including a response to field components normal to the axes of the model.

It was recognized that models that combine the efficiency of the Preisach models and the vector response of the particle assembly models are required for magnetic simulations of vector hysteresis processes. In [49] and [45] a composite of

scalar Preisach and particle assembly modelling in which the asteroids, see also Fig.9, of the Stoner-Wohlfarth model [42] replace the simple rectangular loops of the scalar Preisach model and are shifted to represent interactions. Indeed, it was assumed that each point in the Preisach plane represents the average behaviour of a certain group of real particles in the medium, i.e. each point in the Preisach plane corresponds to a pseudo particle of the medium. In that case, each point in the Preisach space is defined by the two switching fields α and β and two angles (a polar angle and an azimuthal angle in a spherical coordinate system) defining the orientation of the pseudo particle. Connecting the Preisach model and the Stoner-Wohlfarth model resulted in combining moving domain walls processes with the intrinsic rotation of the domain walls. In [50] a straightforward identification procedure for combined Preisach – Stoner-Wohlfarth vector hysteresis models has been presented.

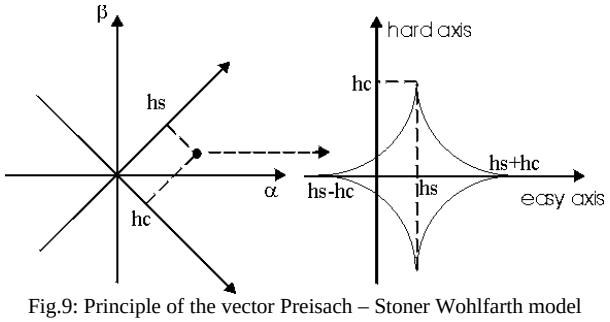

Fig.9: Principle of the vector Preisach – Stoner Wohlfarth model

A memory mechanism was postulated by Mayergoyz [19], and used in its vector Preisach model, designed as the extension of the classical Preisach model. This model is however computationally intensive [51]. In [52] a specific property of the 'Mayergoyz' vector hysteresis model was discussed, the so called 'spiral reduction' property or the wipe-out memory property: two line segments that subtend a part of the magnetic field locus can be used to replace this part of the locus without change in the current model output (the magnetization vector). This is illustrated in Fig. 10.

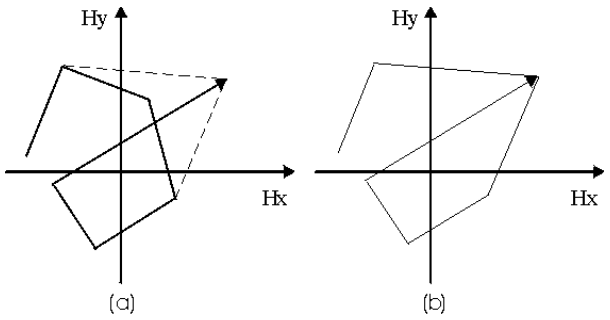

Fig.10: (a) Original magnetic field input curve (full line) with two dotted lines subtending a part of it from the current input point (b) Relevant input magnetic field –locus after wiping-out

In [53], this vector form of wipe out memory was tested experimentally for particulate iron oxide magnetic medium using a vibrating sample magnetometer by generating magnetic field trajectories that are self-crossing.

Several other vector hysteresis models have been proposed in the literature [54], [55], [56], [57], [58], [59] but they still have certain limitations. Also dynamic vector hysteresis models have been introduced in [19].

Especially in the case of arbitrary two-dimensional magnetization patterns (i.e. patterns different from circles and ellipses), there is very little information available on the applicability and accuracy of the various models. A major difficulty hereby is the determination of the actual memory state of the material depending on the history of the magnetic excitation.

VII. Neural Network Scalar Hysteresis Models

The finite element analysis of electromagnetic devices is a commonly used design tool. Critical to this process is the development of effective material models. During the non-linear finite element iteration process, it is necessary to evaluate the appropriate *MH* or *BH* relationship many times for each element. Thus there is a requirement for a hysteresis modelling approach that is both memory efficient and fast. In case of unidirectional magnetization, i.e. $\underline{H}(t)$ and $\underline{B}(t)$ are scalars, denoted $H(t)$ and $B(t)$), one of the most widely used models for magnetic hysteresis is the Preisach model. However, the extension of the model to two-dimensional (e.g. circular) magnetization, as occurring in the laminations of rotating electrical machines, but also to a less extent in transformers, is not straightforward [19]. "Black box" input-output mathematical models, based on artificial neural networks (ANN) [60], are emerging as a powerful modelling tool and could form an alternative to hysteresis modelling techniques like the Preisach model.

Several authors have considered the use of an artificial neural network as a method of providing a functional representation of the hysteresis curve whilst minimizing the storage and time requirements [61], [62].

Artificial neural networks (ANN) are "black box" mathematical tools that can be used for modelling non-linear dynamic input-output relations [60]. The outputs y_l of such a network are determined as weighed sums of its inputs u_i, combined with a non-linear sigmoidal activation function g (a linear activation $\tilde{g}$ is used for the output layer and one hidden layer):

$$y_l = \tilde{g}\left(\sum_{j=0}^{N} w_{lj}^{(2)} g\left(\sum_{i=0}^{n} w_{ji}^{(1)} u_i\right)\right) \qquad l = 0,1,\ldots,m \quad (9)$$

The weights $w_{ij}^{(k)}$ are determined by network training [60]. A theorem states that any continuous non linear function f of an arbitrary number of variables can be approximated arbitrary well over a compact interval by a multilayer Feed-Forward Neural Network (FFNN) consisting of one or more hidden layers, provided the number of hidden units is sufficiently large [60].

During the design of the neural network model, the design of the input vector is critical. If the inputs are not independent then the training time for the neural network can increase with little benefit in the modelling. If the input set is not complete then the result will not provide an accurate representation of the system. The performance of a neural network is determined both by its architecture and the values of the weights associated with the inputs and output of each neuron. The weights are found through a training process in which the network is presented with a large number of sets of the input data and corresponding outputs. The weights are adjusted until the trained response of the network matches the desired response. The set of available data is usually broken into two parts: the first for the actual training, the second for testing the performance of the trained network. In general a classical feed forward neural network is used in literature, trained using error back propagation.

In [63] the chosen input vector of the neural network for one space component of H consists of 5 variables: the previous

(M,H) pair, the current (M,H) pair and the next H. The output is the next value of M. This type of neural networks is good for the description of scalar limit hysteresis cycles but has its limitations for modelling minor order loops.

The approaches described in [64] and [65] are based on the assumption that one can reasonably describe the memory mechanism in systems with rate-independent hysteresis through Preisach state updating rules. Then, the resulting neural model is constituted by two blocks. The first one is a memory block while the second one is a feed forward neural network. The model identification consists then in training the neural network. In [65] one uses the Preisach dipole formalism in the memory block while in [64] the memory block contains play operators. The disadvantage of these neural models is the large number of inputs (number of Preisach dipoles - number of play operators).

In [66] a neural network hysteresis model that offers the same accuracy as the classical scalar Preisach model was presented. The neural network topology and input parameters are chosen based on the properties of the Preisach model and the theory of dynamic systems. Two important properties of the classical scalar Preisach model [19] are taken into account for the development of the neural network model. Firstly, the Preisach model describes rate-independent (quasi-static) hysteresis. Indeed, the hysteresis memory state at each time step k is determined only by the extreme values (maxima and minima) of the field strength history H_0, H_1, …, H_{k-1}, H_k, The change of the magnetic induction B_k (the model output) is determined from the current field value H_k and exactly one stored extreme field value H_k^{extr}, at each time step k (Fig. 11). The relevant extreme value H_k^{extr} is the last one stored in memory. The closing of a minor loop deletes from memory the maximum and minimum H-values associated with this minor loop (the wiping-out property [19]. When no extreme values are present in memory, the virgin magnetization curve is followed. The relevant extreme value H_k^{extr}can be determined at each time step k by an algorithm that stores the encountered extreme values and implements the wiping-out property. The second important property of the classical Preisach model is the congruency property. It states that BH-loops between two fixed extreme field values are independent of the induction level B.

Combining the two properties, the classical scalar Preisach model can be expressed mathematically as:

$$B_k = B_k^{extr} + f\left(H_k^{extr}, H_k, FLAG_k\right) \qquad (10)$$

where B_k^{extr} is the corresponding induction level at the relevant extreme field value H_k^{extr} and f is a nonlinear function of three variables. The variable $FLAG_k$ can take only two different values, e.g. –1 and 1, to distinguish between the virgin curve (no extreme values present in memory) and a hysteresis branch, respectively. Indeed, for the special case $H_k^{extr}=0$, there exist two distinct curves: $B_k=B_k^{extr}+f_1(0,H_k)$ when following the virgin curve ($B_k^{extr}=0$), and $B_k=B_k^{extr}+f_2(H_k^{extr},H_k)$ when following a hysteresis branch. Note that Eq.(10) is similar to the description of the Preisach model with the Everett function $E_v(H_1,H_2)$ [3]:

$$\begin{aligned} B_k - B_k^{extr} &= E_v(H_k^{extr}, H_k) \quad or \\ B_k &= \tfrac{1}{2} E_v(-H_k, H_k) \end{aligned} \qquad (11)$$

depending whether a hysteresis branch or the virgin curve is followed, respectively. Here, $E_v(H_1,H_2)$ is the two dimensional function giving the variation of the magnetic induction when varying the magnetic field from H_1 to H_2, where H_1 or H_2 are extremal values and during the variation no extremal values are wiped out of the memory, see above.

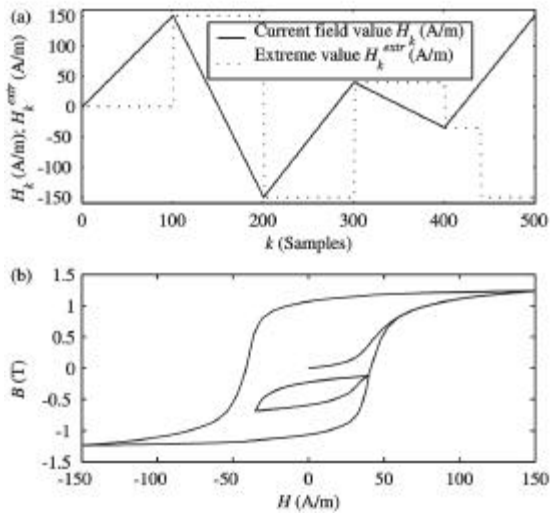

Fig.11: Wiping out (deletion) property of rate-independent hysteresis (a) input sequence and corresponding extreme values; (b) input-output trajectory

With regard to computational efficiency and required training sets, it is convenient to model only the non-linear part of (10), and use:

$$B_k = B_k^{extr} + FFNN_{stat}\left(H_k^{extr}, FLAG_k, H_k\right) \qquad (12)$$

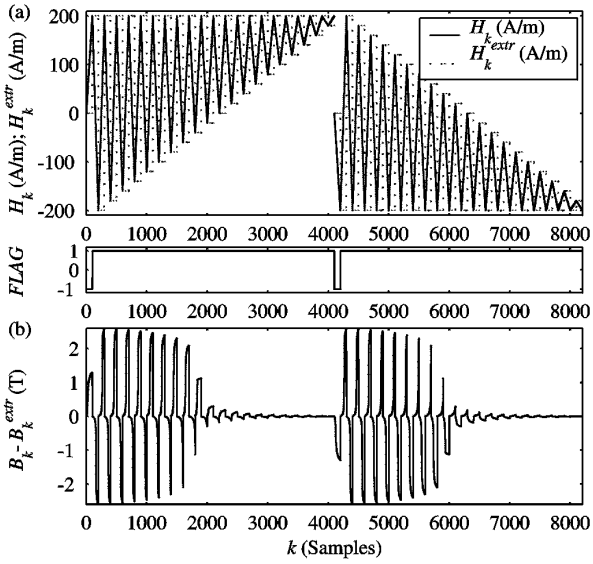

Fig.12: A possible training set for the feed-forward neural network.

Note the similarity with the Everett function description. The $FFNN_{stat}$ fully describes the Everett function $E_v(H_1,H_2)$. In order to use the neural network of Eq.(9) for hysteresis loop prediction, it should be trained, i.e. the weights $w_{ij}^{(k)}$ determined. A suitable training set of known input and output pairs is used for this task. The (measured) training set should span the whole range of possible network input values, because a neural network is capable of performing accurate non-linear interpolations, but is not suitable for extrapolation. For a fixed maximum field strength H^{max}, a possible training set providing all the necessary information is shown in Fig.12. The neural network model was also tested with a test set shown in Fig.13a, which was not used during training. Fig.13b

shows that both major and minor hysteresis loops can be predicted very accurately, thereby proving that the neural network technique is suitable for hysteresis modelling.

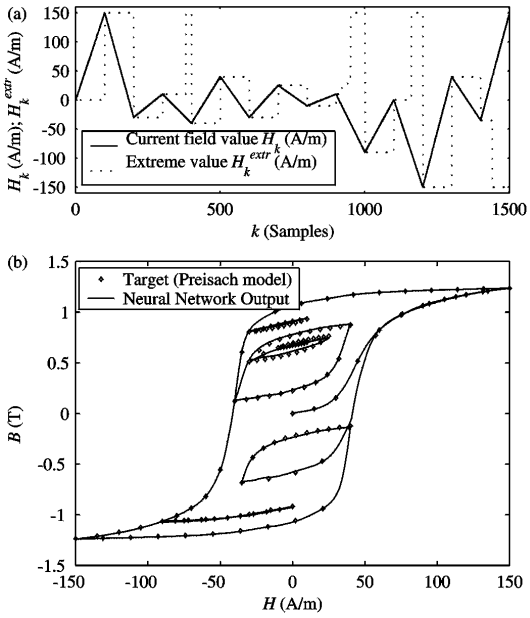

Fig.13: Comparison between congruent loops neural network model and classical Preisach model for FeSi steel: (ainput history) (b) input-output trajectory.

Dynamic hysteresis, or the relation between the time dependent B(t) and $H_{tot}(t)$, can be treated conveniently based on the loss-separation property of SiFe alloys [67]. According to this property, the total power loss of the ferromagnetic lamination can be divided into quasi-static (hysteresis) and dynamic (classical, including skin-effect, and excess) loss components, P_{hyst} and P_{dyn} respectively. The quasi-static field $H_{hyst}(t)$ and the dynamic field $H_{dyn}(t)$, see Fig.7, can be associated with the corresponding loss components for each time point t, leading to Eq.(8) for the instantaneous power loss $P_{tot}(t)$ at time t [67].

The quasi-static and dynamic contributions can thus be treated independently [68]. Using neural networks, (9) suggests combining two feed-forward neural networks (FFNN), one that determines the quasi-static BH_{hyst}-loop and one that yields the dynamic field $H_{dyn}(t)$, for a given B(t) as input. The modelling of quasi-static magnetic hysteresis, which obeys the wiping-out and congruency properties of the classical Preisach model, was presented in the previous section. The system state is determined by the last extreme magnetic field value $H_{hyst}^{extr}(t)$, kept in memory, and the corresponding induction value $B^{extr}(t)$. Both can easily be determined from the magnetic field and induction history. This model can be used to iteratively determine the quasi-static BH_{hyst}-loop for a given B(t).

The dynamic field $H_{dyn}(t)$ depends on the induction B(t) and its rate of change dB/dt [67]., but is assumed not to depend on the magnetization history of the material. The dynamic field $H_{dyn}(t)$ can thus be modelled by a FFNN with 2 inputs:

$$H_{dyn}(t) = FFNN_{dyn}\left(B(t), \frac{dB(t)}{dt}\right) \qquad (14)$$

In order to use the network (14) for the prediction of $H_{dyn}(t)$, it should be trained, i.e. the weights $w_{ij}^{(k)}$ determined. A suitable training set of known input and output pairs is used for this task [60]. The (measured) training set should span the whole range of possible network input values, because a neural network is capable of performing accurate non-linear interpolations, but is not suitable for extrapolation. For the network (14), a possible training set providing all the necessary information consists of the sinusoidal BH_{tot}-loops at saturation, for a set of different frequencies. For each BH_{tot}-loop, the quasi-static BH_{hyst}-loop is calculated by the classical Preisach-model or the neural network model, yielding the dynamic field $H_{dyn}(t)$ and thus the input-output pairs for the training of the network (14). A quasi-static loop at saturation (with dB/dt and $H_{dyn}(t)$ identically zero) is included in the training set to improve the network performance for low values of dB/dt. The number of different frequencies that should be used, as well as the number of elements in the hidden layer of the neural network, are determined experimentally to ensure the generalization capability of the network and avoid overfitting [60]. A set of test loops, different from the training loops, is used to investigate the network performance.

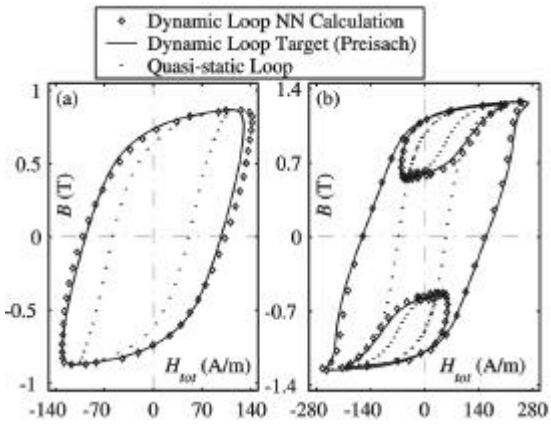

Fig.14: Comparison between FFNN prediction and results from Preisach model: (a) sinusoidal magnetization at 0.87 T, 100 Hz; (b) sinusoidal magnetization at 50Hz, distorted with third and fifth harmonics.

In order to test the proposed approach, a measured training set was used. A feed-forward neural network with 10 neurons was trained with loops for only 6 different frequencies from 50 Hz to 400 Hz, using the Levenberg-Marquardt training algorithm [60]. for 200 epochs (iterations). The accuracy of the results for all the test loops is good. For the loops at saturation, the error for the calculated power loss is less than 1 % above 50 Hz. The saturation loops below 50 Hz as well as the loops at lower induction levels and for distorted waveforms yield higher deviations in the loss values, up to 10 %. Fig.14 shows typical results. The reduced accuracy for lower inductions suggests that the maximum induction B_{max} in the BH_{tot}-loop slightly affects the dynamic field $H_{dyn}(t)$.

In [69], three versions of a vector hysteresis model for electrical steel sheets are presented, based on the function approximation capabilities of feed-forward neural networks and the memory mechanism of vector hysteresis proposed by Mayergoyz [19]. In the memory mechanism postulated by Mayergoyz, the past extrema $H_{y,k}^{extr}$ of the projections of the input vector $\underline{H}_k$ along all possible directions y in the plane of the sheet may influence the future evolution of the output $\underline{B}_k$ and thus contain the vector memory state of the material

The first model handles arbitrary vector magnetization patterns, but requires a very extended data set for the training of the neural network. The second model is suitable for convex induction loci and allows a reduction of the required training set. The third model handles the features of the considered magnetization pattern in an alternative way and relaxes the convexity requirement. The choice of the specific

model, its parameters and the network training set depends on the types of magnetization patterns concerned. Arbitrary high accuracy can be reached by extending the complexity of the model and/or the size of the training set. Experimental results for the third model are presented and show the good accuracy of the approach. Standard neural network algorithms are used.

In these vector hysteresis models, both field vectors are restricted to vary in the plane of the laminated SiFe steel and are denoted $\underline{H(t)}$=|H(t)|exp(jφ^{H}(t)) and $\underline{B(t)}$=|B(t)|exp(jφ^{B}(t)), see Fig.15a. A FFNN model for arbitrary vector magnetization patterns, resolving the limitations of the Preisach-Mayergoyz model, can be constructed as follows. The inputs of the FFNN at each time step k are the amplitude $|H_k|$ and phase j_k^H of the field strength $\underline{H}_k$, along with the relevant extrema $H_{yp,k}^{extr}$ of the projections of $\underline{H}_k$ and the corresponding $B_{yp,k}^{extr}$ along a set of P directions y_p, p = 1, …, P. The outputs of the FFNN are the induction amplitude $|B_k|$ and the lag angle q_k (see Fig.15.a):

$$\left(|B_k|, q_k\right) = FFNN_{stat}\left(|H_k|, j_k^H, H_{y_1,k}^{extr}, B_{y_1,k}^{extr}, \ldots, H_{y_P,k}^{extr}, B_{y_P,k}^{extr}\right) \quad (15)$$

Note that this model 1 is an extension of the Preisach-Mayergoyz model, as it takes the complete memory state of the material into account in the limit of an infinite number of directions y. The model is thus capable of approximating the relation between $\underline{H}_k$ and $\underline{B}_k$ for arbitrary vector magnetization patterns, provided the memory mechanism of Mayergoyz correctly determines the memory state of the material. The approximation accuracy of the model is increased by using a denser set of directions y. A major practical disadvantage of this method is that the FFNN requires a very extensive training set, consisting of experimental data spanning the whole range of possible magnetization patterns, including various combinations of vector minor loops. However, if one disposes of such an extensive training set and the FFNN is trained correctly, it can yield a very accurate vector hysteresis model.

The previous method has the additional disadvantage that the measurement of the magnetization patterns for the training set is mostly performed under the condition of a controlled induction waveform on a Rotational Single Sheet Tester (RSST). It is thus difficult to obtain experimental data for predetermined field strength patterns and we would therefore prefer a model with $\underline{B}_k$ as input and $\underline{H}_k$ as output. In the case of convex vector induction patterns such a B-to-H model can be constructed in a way analogous to the already discussed H-to-B model. The convex vector induction patterns do not yield minor loops in the projection on any direction y. In this case each extreme field value $H_{y,k}^{extr}$ corresponds to a unique extreme induction value $B_{y,k}^{extr}$. We can thus construct a FFNN with inputs $|B_k|$ and φ$_k^B$, along with the values $B_{yp,k}^{extr}$ for a set of P directions y_p (Fig.15.b). The outputs of the FFNN are $|H_k|$ and q_k:

$$\left(|H_k|, q_k\right) = FFNN_{stat}\left(|B_k|, j_k^B, B_{y_1,k}^{extr}, \ldots, B_{y_P,k}^{extr}\right) \quad (16)$$

This model 2 yields an arbitrary accurate vector hysteresis model for convex induction patterns. The training of the FFNN should use an extended set of such convex patterns. Note that a training with circular and elliptical magnetization patterns only is not correct. In such a case the FFNN would not be able to calculate accurately any pattern different from a circle or an ellipse.

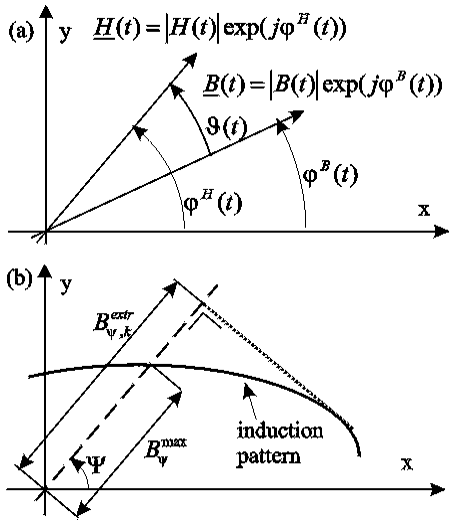

Fig.15: Notations: (a) $\underline{B}$(t) and $\underline{H}$(t) in lamination plane; (b) $B_{yp,k}^{extr}$ and $B_{yp,k}^{max}$ for an induction pattern

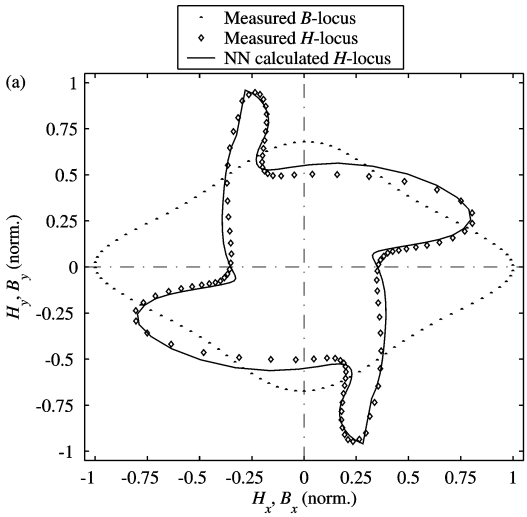

Fig.16: Measured and calculated $\underline{H}_k$ and $\underline{B}_k$ for patterns from the test set of the FFNN $|B|_{max}$=1T; $|H|_{max}$=105 A/m

In order to relax the requirement for convex induction patterns, we note that we can take hysteresis memory into account in an alternative way, using as inputs of the FFNN the specific features of each considered induction pattern. In particular, the maximum values B_{yp}^{max} of $|B_k|$ along a set of P directions y_p (Fig.15b), along with information about the direction of rotation of the induction pattern (clockwise or counter clockwise), contain sufficient information about the considered pattern in the case there are no vector minor loops. This data can thus be used as inputs of the FFNN instead of $B_{yp,k}^{extr}$. Note that in the limit of an infinite number of different directions y, these values B_y^{max} uniquely determine the induction pattern for a known direction of rotation. The training of the FFNN of this model 3 uses again an extended set of measured magnetization patterns. Note that one can adapt the complexity of this vector hysteresis model depending on the required accuracy of the application or the specific types of the considered induction patterns, for example by reducing or increasing the number P of directions y_p. These models were experimentally verified in [69]. Some results are shown in Fig. 16.

In [70], a dynamic vector hysteresis model based on neural networks, was presented, based on the loss separation property of SiFe steels [67]:

$$P_{tot}(t) = P_{hyst}(t) + P_{dyn}(t) = \frac{d\underline{B}(t)}{dt}.\underline{H}_{tot}(t) =$$
$$\frac{dB_x(t)}{dt}\left(H_{hyst,x}(t) + H_{dyn,x}(t)\right) + \quad (17)$$
$$\frac{dB_y(t)}{dt}\left(H_{hyst,y}(t) + H_{dyn,y}(t)\right)$$

The time dependent field at the surface of the lamination is denoted $\underline{H}_{tot}(t) = H_{tot,x}(t)\,\underline{1}_x + H_{tot,y}(t)\underline{1}_y$ and the induction averaged out over the cross section of the lamination is $\underline{B}(t) = B_x(t)\underline{1}_x + B_y(t)\underline{1}_y$, with t the time, in Cartesian representation. As in the scalar case, $\underline{H}_{dyn}(t) = H_{dyn,x}(t)\,\underline{1}_x + H_{dyn,y}(t)\underline{1}_y$ is modeled with a suitable additional feed-forward neural network.

VIII. Finite element formulations

The industrial characterisation of soft magnetic materials is based on measurements performed on laminations packed inside an Epstein frame under imposed sinusoidal flux conditions. The actual operating conditions of the material inside an electromagnetic device are far from those reproduced on Epstein frame: distorted flux patterns are very often found inside devices, due to saturation, slot effects and non-sinusoidal electronic supply systems. The capability to numerically simulate the complicated conditions could give an important tool for a deeper insight into iron losses. A possible approach to the analysis of the phenomena inside the ferromagnetic laminations is to describe the interacting hysteresis and eddy current effects in terms of the macroscopic fields. This is performed by means of numerical methods for the solution of Maxwell equations in magnetic cores combined with advanced hysteresis models, described above. The corresponding 1D-diffusion problems in laminated structures are described in detail in e.g. [71], [72], [73], [74].

In the conventional magnetic field analyses that are applied for the design of electromagnetic devices, the magnetic properties have been modelled by simplified material models.

There has been publications [75], [76] [77] were hysteresis models were included in 2D finite element analysis. However, the material models are scalar models, even though the electromagnetic field analysis with ferromagnetic materials needs a 2D or even a 3D vector hysteresis modelling.

In [78] a numerical scheme was proposed in order to include the modelling of the two-dimensional magnetic properties using the magnetic reluctivity tensor.

In [79] a 2D vector hysteresis model using the play and stop hysteron models is presented and included in 2D eddy current finite element analysis. The play and stop hysteron theory allows to construct a hysteresis model with the B-vector as input, which simplies the finite element scheme when using a vector potential formulation.

In [80] the finite element computations taking into account the materials properties by the Mayergoyz vector hysteresis model have been verified experimentally by comparing the numerical results with measurements on a transformer type device. Also neural network hysteresis modelling has been included in finite element analysis, see e.g. [81].

IX. Conclusions

The finite element analysis of electromagnetic devices may require a computationally efficient material hysteresis model describing the time-dependent non-linear relation between the magnetic field strength vector $\underline{H}(t)$ and the magnetic induction vector $\underline{B}(t)$, both under unidirectional and two-dimensional magnetization. Without claiming completeness, this paper gives an overview of scalar and vector hysteresis models studied and discussed in the past. Physical based and phenomenological hysteresis models were considered. Mathematical models, based on artificial neural networks, could form an alternative to e.g. Preisach-type hysteresis models, resulting in substantial savings of computation time.

The development of general purpose numerical schemes for solving Maxwell's equations in 2 and 3 dimensions in combination with complex constitutive laws describing vector hysteresis properties is probably one of the challenges for the next few years. Here, the Compumag community may play an important role.

X. References

[1] Mandelung E., "On the magnetization by a fast current and an operation principle of the magnetodetectors of Rutherford-Marconi", *Ann. Phys.*, vol. 17, 1905, pp.861-890.

[2] Preisach F., "Uber die magnetische Nachwirkung", *Zeitschrift fur Physik*., vol. 94, 1935, pp. 277-302.

[3] Everett D., "A general approach to hysteresis IV: An alternative formulation of the domain model", *Trans. Faraday Society*, vol. 51, 1955, pp.1551-1557.

[4] Park G., Hahn S., "Implementation of hysteresis characteristics using the preisach model with MB variables", *IEEE Trans. on Magn.*, vol. 29, 1993, pp. 1542-1545.

[5] Dupré L., Van Keer R., Melkebeek J., "Modelling and identification of the iron losses in non-oriented steel laminations using the Preisach theory", *IEE Proc. - Electric Power Appl.*, vol. 144, 1997, pp. 227-234.

[6] Bertotti G., Fiorillo F., Soardo G., "The prediction of power losses in soft magnetic materials", *J. Phys.*, vol. 49, 1988, pp. 1915-1919.

[7] Della Torre E., Vajda F., "Properties of accomodation models", *IEEE Trans. on Magn*., vol. 31, 1995, pp. 1775-1780.

[8] Della Torre E., Kadar G., "Hysteresis modelling: II Accomodation", *IEEE Trans. on Magn*., vol. 23, 1987, pp. 2823-2825.

[9] Vadja F., Della Torre E., "Relationship between the moving and the product Preisach models", *IEEE Trans. on Magn*., vol. 27, 1991, pp. 3823-3826.

[10] Vadja F., Della Torre E., "Measurements of output dependent Preisach functions", *IEEE Trans. on Magn.*, vol. 27, 1991, pp. 4757-4762.

[11] Bertotti G., Basso V., "Considerations on the physical interpretation of the Preisach model of ferromagnetic hysteresis", *J. Appl. Phys*., vol. 73, 1993, pp. 5827-5829.

[12] Basso V., Bertotti G., "Description of magnetic interactions and Henkel plots by the Preisach model", *IEEE Trans. on Magn.*, vol. 30, 1994, pp. 64-72.

[13] Henkel G., "Remanenzverhalten und wechselwirkungen in hartmagnetischen Teilchenkollektiven", *Phys. Status Solidi*, vol.7, 1964, pp. 919-929.

[14] Vajda F., Della Torre E., Pardavi-Horvath M., "Analysis of the reversible magnetization dependent Preisach models for recording media", *J. Magn. Magn. Mat.*, vol. 115, 1992, pp. 187-189.

[15] Della Torre E., Vajda F.,"Parameter identification of the complete moving hysteresis model using major loop

data", *IEEE Trans. on Magn*., vol. 30, 1994, pp. 4987-5000.
[16] Kadar G., Kisdi-Koszo E., Kiss L., Potocky L., Zatroch M., Della Torre E., "Bilinear product Preisach modelling of magnetic hysteresis curves", *IEEE Trans. on Magn.*, vol. 25, 1989, pp. 3931-3933.
[17] Kadar G. "On the product Preisach model of hysteresis", *Physica B*, vol. 275, 2000, pp. 40-44.
[18] Basso V., "Hysteresis and relaxation effects in magnetic materials", *IEEE Trans. on Magn*., vol. 36, 2000, pp. 3176-3181.
[19] Mayergoyz I., *Mathematical models of hysteresis*, Springer Verlag, 1991.
[20] Korman C., Mayergoyz I., "Preisach model driven by stochastic inputs as a model for after effect", *IEEE Trans. on Magn*., vol. 32, 1996, pp. 4204-4209.
[21] Hodgdon M., "Application of a theory of ferromagnetic hysteresis", *IEEE Trans. on Magn*., vol. 24, 1988, pp. 218-221.
[22] Jiles D. C. and Atherton D. L., "Theory of ferromagnetic hysteresis", *J. Magn. Magn. Mat*., vol. 61, 1986, pp. 48-60.
[23] Sablik M.J. and Jiles D.C., "Coupled magnetoelastic theory of magnetic and magnetostrictive hysteresis", *IEEE Trans. on Magn*., vol. 29, 1993, pp. 2113- 2123.
[24] Jiles D., Atherton D., "Ferromagnetic hysteresis", *IEEE Trans. on Magn.*, vol. 19, 1983, pp. 2183-2185.
[25] Jiles D., Thoelke J., Devine K., "Numerical determination of hysteresis parameters for the modelling of magnetic properties using the theory of ferromagnetic hysteresis", *IEEE Trans. on Magn*., vol. 28, 1992, pp. 27-35.
[26] Jiles D., "A self consistent generalized model for the calculation of minor loop excursions in the theory of hysteresis", *IEEE Trans. on Magn.*, vol. 28, 1992, pp. 2602-2604.
[27] Pasquale M., Basso V., Bertotti G., Jiles D., Bi Y., "Domain wall motion in random potential and hysteresis modeling", *J. of Appl. Phys*., vol. 83, 1998, pp. 6497-6499.
[28] Jiles D., "Frequency dependence of hysteresis curves in non conducting magnetic materials", *IEEE Trans. on Magn*., vol. 29, 1993, pp. 3490-3492.
[29] Jiles D., *Introduction to magnetism and magnetic materials.*, Chapman & Hall, 1991.
[30] Bertotti G., "Dynamic generalization of the scalar Preisach model of hysteresis", *IEEE Trans. on Magn.*, vol. 28, 1192, pp. 2599-2601.
[31] Bertotti G., "Generalized Preisach model for the description of hysteresis and eddy current effects in metallic ferromagnetic materials", *J. of Appl. Phys.*, vol. 69, 1991, pp. 4608-4610.
[32] Bertotti G., "Generalized properties of power losses in soft ferromagnetic materials", *IEEE Trans. on Magn.*, vol. 24, 1988, pp. 621-630.
[33] Dupré L., Bertotti G., Melkebeek J., "Dynamic Preisach model and energy dissipation in soft magnetic materials", *IEEE Trans. on Magn.*, vol. 34, 1998, pp. 1168-1170.
[34] Bertotti G., Pasquale M., "Physical interpretation of induction and frequency dependence of power losses in soft magnetic materials", *IEEE Trans. on Magn.*, vol. 28, 1992, pp. 2787-2789.
[35] Bertotti G., "Space time correlation properties of the magnetization process and eddy current losses, Applications I: fine wall spacing ", *J. of Appl. Phys.*, vol. 55, 1984, pp. 4339-4347.
[36] Dupré L., Van Keer R., Melkebeek J., "Dynamic hysteresis model for $f^{1/(1+s)}$ excess loss dependence", *J. of Mat. Proc. and Manuf. Science*, vol. 9, 2001, pp. 4-13.
[37] Dupré L., Bertotti G., Basso V., Fiorillo F., Melkebeek J., "Generalisation of the dynamic Preisach model towards grain oriented SiFe alloys", *Physica B*., vol. 275, 2000, pp. 202-206.
[38] Chevalier T., Kedous-Lebouc A., Cornut B., Cester C., "A new dynamic hysteresis model for electrical steel sheet", *Physica B*, vol. 275, 2000, pp. 197-201.
[39] Dupré L., Van Keer R., Melkebeek J., "Modelling the electromagnetic behaviour of SiFe alloys using the Preisach theory and the principle of loss seperation", *Math. Probl. in Eng*., vol. 7, 2001, pp. 113-128.
[40] Suzuki K., "Theoretical study of vector magnetization distribution using rotational magnetization model", *IEEE Trans. on Magn.*, vol. 12, 1976, pp. 224-229.
[41] Ortenburger I., Potter R., "Self-consistent calculation of the transition zone in thick particulate recording media", *J. of Appl. Phys.*, vol.50, 1979, pp. 2393-2395.
[42] Stoner E., Wohlfarth E., "A mechanism of magnetic hysteresis in heterogeneous alloys", *IEEE Trans. on Magn*., vol. 27, 1991, pp. 3475-3518.
[43] Mayergoyz I., "Mathematical models of hysteresis", *IEEE Trans. on Magn*., vol. 22, 1986, pp. 603-608.
[44] Pinto M., "Vectorial aspects of ferromagnetic hysteresis", *J. Magn. Magn. Mat.*, vol. 98, 1991, pp. 221-229.
[45] Cramer H., "A moving Preisach vector hysteresis model for magnetic recording media", *J. Magn. Magn. Mat.*, vol. 88, 1990, pp. 194-204.
[46] Adly A., Mayergoyz I., "A new vector Preisach type model of hysteresis", *J. of Appl. Phys*., vol. 73, 1993, pp. 5824-5826.
[47] Wiesen K., and Charap H., "Vector hysteresis modelling", *J. of Appl. Phys*., vol. 61, 1987, pp. 4019-4021.
[48] Wiesen K., Charap H., Krafft S., "A rotational vector Preisach model for unoriented media", *J. of Appl. Phys.*, vol. 67, 1990, pp. 5367-5369.
[49] Oti J., Della Torre E., "A vector moving model of both reversible and irreversible magnetization processes", *J. of Appl. Phys.*, vol. 67, 1990, pp. 5364-5366.
[50] Ossart F., Davidson R., Charap S., "A 3D moving vector Preisach hysteresis model", *IEEE Trans. on Magn.*, vol. 32, 1995, pp. 1785-1788.
[51] Ragusa C., Repetto M., "Accurate analysis of magnetic devices with anisotropic vector hysteresis", *Physica B*, vol. 275, 2000, pp. 92-98.
[52] Friedman G., "Conditions for the representation of vector hysteresis by the vector Preisach model", *J. of Appl. Phys*., vol. 85, 1999, pp. 4379-4381.
[53] Friedman G., Cha K., Huang Y., Kouvel J., "Vector form of wipe-out memory and its experimental testing", *IEEE Trans. on Magn.*, vol. 36, 2000, pp. 3185-3188.
[54] Della Torre E., "A simplified vector Preisach model", *IEEE Trans. on Magn.*, vol. 34, 1998, pp. 495-501.
[55] Vernescu-Spornic C., Kedous-Lebouc A., Spornic S., Ossart F., "Anisotropic and vector hysteresis model for magnetic materials applications to a cubic textured NiFe sheet", *Physica B*, vol. 275, 2000, pp. 99-102.
[56] Bergqvist A., "A simple vector generalization of the Jiles-Atherton model of hysteresis", *IEEE Trans. on Magn.*, vol. 32, 1996, pp. 4213-4215.
[57] Kedous-Lebouc A., Vernescu C., Cornut B., "A two-dimensional Preisach particle for vectorial hysteresis modeling", *J. Magn. Magn. Mat*., vol. 254, 2003, pp. 321-323.

[58] Appino C., Valsania M., Basso V., "A vector hysteresis model including domain wall motion and coherent rotation", *Physica B*, vol. 275, 2000, pp. 103-106.
[59] Stancu A., Spinu L., "Temperature and time-dependent Preisach model for a Stoner Wohlfarth particle system", *IEEE Trans. on Magn.*, vol. 34, 1998, pp. 3867-3875.
[60] Bishop C., *Neural Networks for Pattern Recognition*, Oxford Univ. Press, 1995.
[61] Nafalski A., Hoskins G., Kundu A., Doan T., "The use of neural networks in describing magnetisation phenomena", *J. Magn. Magn. Mat.*, vol. 160, 1996, pp. 84-86.
[62] Mandayam D., Upda L., Upda S., "Parametric models for representing hysteresis curves", *Nondestr. Testing Evaluation*, vol. 11, 1994, pp. 235-245.
[63] Saliah H., Lowther D., "Modelling magnetic materials using artificial neural networks", *IEEE Trans. on Magn.*, vol. 34, 1998, pp. 3056-3059.
[64] Serpcio C., Visone C., "Magnetic hysteresis modelling via feed-forward neural networks", *IEEE Trans. on Magn.*, vol. 34, 1998, pp. 623-628.
[65] Adly A., Abd-El-Hafiz S., "Using neural networks in the identification of Preisach type hysteresis models", *IEEE Trans. on Magn.*, vol. 34, 1998, pp. 629-635.
[66] Makaveev D., Dupré L., De Wulf M., Melkebeek J., "Modelling of quasi-static magnetic hysteresis with feed-forward neural networks", *J. of Appl. Phys.*, vol. 89, 2001, pp. 6737-6739.
[67] Bertotti G., *Hysteresis in Magnetism*, Academic Press, 1998.
[68] Chevalier T., Kedous-Lebouc A., Cornut B., Cester C., "A new dynamic hysteresis model for electrical steel sheet", *Physica B*, vol. 275, 2000, pp. 197-210.
[69] Makaveev D., Dupré L., De Wulf M., Melkebeek J., "Combined Preisach 'Mayergoyz' neural network vector hysteresis model for electrical steel sheets", *J. of Appl. Phys.*, vol. 93, 2003, pp. 6638-6640.
[70] Makaveev D., Dupré L., Melkebeek J., "Neural network based approach to dynamic hysteresis for circular and elliptical magnetization in electrical steel sheet", *IEEE Trans. on Magn.*, vol. 38, 2002, pp. 3189-3191.
[71] Del Vecchio R., "An efficient procedure for modelling complex hysteresis processes in ferromagnetic materials", *IEEE Trans. on Magn.*, vol. 16, 1980, pp. 809-811.
[72] Miano G., Serpico C., Verolino L., Visone C., "Comparison of different hysteresis models in FE analysis of magnetic field diffusion", *IEEE Trans. on Magn.*, vol. 31, 1995, pp. 1789-1792.
[73] Dupré L., Bottauscio O., Chiampi M., Repetto M., Melkebeek J., "Modelling of electromagnetic phenomena in soft magnetic materials under unidirectional time periodic flux excitations", *IEEE Trans. on Magn.*, vol. 35, pp. 4147-4184.
[74] Dupré L., Van Keer R., Melkebeek J., "Complementary 2D finite element procedures for the magnetic field analysis using a vector hysteresis model", *Intern. J. for Num. Meth. in Eng.*, vol. 42, 1998, pp. 1005-1023.
[75] Takahashi N., Miyabara S., Fujiwara K., "Problems in practical finite element analysis using Preisach model", *IEEE Trans. on Magn.*, vol. 35, 1999, pp. 1243-1246.
[76] Park G., Hahn S., Lee S., Jung H., "Implementation of hysteresis characteristics using the Preisach model with MB-variables", *IEEE Trans. on Magn.*, vol. 29, 1993, pp. 1542-1545.
[77] Gyselinck J., Dupré L., Vandevelde L., Melkebeek J., "Calculation of no load induction motor core losses using the rate dependent Preisach model", *IEEE Trans. on Magn.*, vol. 34, 1998, pp. 3876-3881.
[78] Enokizono M., Yuki K., Kanao S., "Magnetic field analysis by finite element method taking rotational hysteresis into account", *IEEE Trans. on Magn.*, vol. 30, 1994, pp. 3375-3378.
[79] Matsuo T., Osaka Y., Shimasaki M., "Eddy current analysis using vector hysteresis models with play and stop hysterons", *IEEE Trans. on Magn.*, vol. 36, 2000, pp. 1172-1177.
[80] Bottauscio O., Chiampi M., Ragusa C., Rege L., Repetto M., "A test case for validation of magnetic field analysis with vector hysteresis", *IEEE Trans. on Magn.*, vol. 38, 2002, pp. 893-896.
[81] Saliah H., Lowther D., Forghani B., "Generalized material models for coupled magnetic analysis", *IEEE Trans. on Magn.*, vol. 36, 2000, pp. 1250-1253.

AUTHORS NAME AND AFFILIATION

Luc Dupré, Department of Electrical Energy, Systems and Automation (EESA),
Sint-Pietersnieuwstraat 41, B-9000 Ghent, Belgium, + 32 9 264 34 24 luc.dupre@ugent.be

Jan Melkebeek, Department of Electrical Energy, Systems and Automation (EESA),
Sint-Pietersnieuwstraat 41, B-9000 Ghent, Belgium, Tel. + 32 9 264 34 17, jan.melkebeek@ugent.be